Valorization of Sarawak Rice Husk: Synthesis and Characterization of Enhanced Purity Amorphous Silica *via* Hydrochloric Acid Leaching

Nur-Azzah Afifah Taib,[a] Md. Rezaur Rahman,[a,]* Khairul Anwar Mohamad Said,[a] Anjelina Joffery Kalimuthu,[a] Ervina Junaidi,[a] Jamal Uddin,[b] Al-Khalid bin Hj Othman,[a] Sulaiman Y. M. Alfaifi,[c] K. S. Alblawi,[c] Maha G. Batterjee,[d] and Mohammed Muzibur Rahman [e]

* *Corresponding author: rmrezaur@unimas.my*

DOI: 10.15376/biores.21.3.7192-7210

GRAPHICAL ABSTRACT

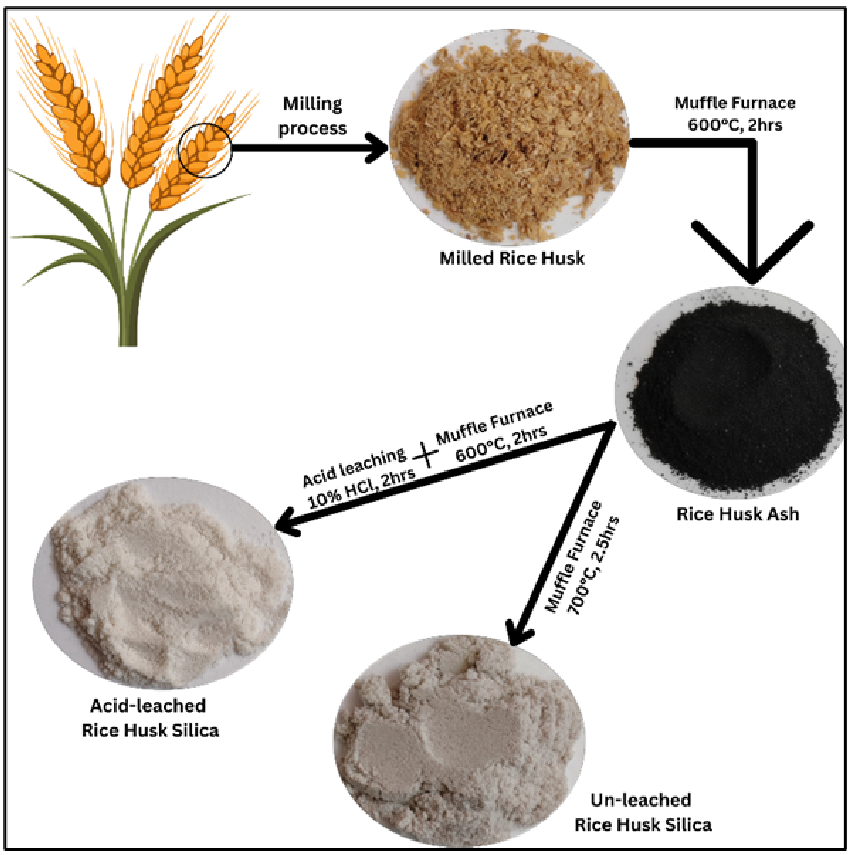

Valorization of Sarawak Rice Husk: Synthesis and Characterization of Enhanced Purity Amorphous Silica *via* Hydrochloric Acid Leaching

Nur-Azzah Afifah Taib,[a] Md. Rezaur Rahman,[a,*] Khairul Anwar Mohamad Said,[a] Anjelina Joffery Kalimuthu,[a] Ervina Junaidi,[a] Jamal Uddin,[b] Al-Khalid bin Hj Othman,[a] Sulaiman Y. M. Alfaifi,[c] K. S. Alblawi,[c] Maha G. Batterjee,[d] and Mohammed Muzibur Rahman [e]

Rice husk (RH) is a global agricultural byproduct that poses environmental challenges due to disposal *via* open burning. This study contributes new findings on the RH valorization from Roban, Sarawak, establishing a highly effective hydrochloric acid (HCl) leaching protocol that yields amorphous silica with enhanced purity. The scientific significance lies in the successful optimization of treatment parameters to achieve superior silica oxide (SiO_2) purity of 97.26 wt%, and significantly enhanced whiteness index (WI) (74.4), demonstrating the efficiency of this protocol for regional variants. Furthermore, the structural analysis demonstrates the isolation of a predominantly amorphous phase, providing a critical baseline for utilizing Sarawak-specific agricultural waste in high-performance industrial applications. Energy dispersive X-ray (EDX) spectroscopy analysis confirmed the successful elimination of metallic impurities (P, K, Ca, and Fe), resulting in a reduced mass yield from 43.18% to 36.64%. Furthermore, HCl treatment narrowed the particle size distribution (SPAN: 1.66) and slightly reduced the mean diameter to 33.0 μm. X-ray diffraction (XRD) and Fourier transform infrared (FTIR) analyses confirmed that both samples retained a stable amorphous structure. These results demonstrate that RH from this region is a viable, low-cost precursor for high-quality silica production, offering a sustainable alternative for agricultural waste management.

DOI: 10.15376/biores.21.3.7192-7210

Keywords: Rice husk (RH); Agricultural waste; Amorphous silica; Acid leaching; Hydrochloric acid (HCl)

*Contact information: a: Department of Chemical Engineering, Faculty of Engineering, Universiti Malaysia Sarawak, 94300, Kota Samarahan, Sarawak, Malaysia; b: Center for Nanotechnology, Department of Natural Sciences, Coppin State University, Baltimore, MD, USA; c: Department of Chemistry, King Abdulaziz University, Jeddah 21589, Saudi Arabia; d: Center of Excellence for Advanced Materials Research, Faculty of Science, King Abdulaziz University, Jeddah 21589, Saudi Arabia; *Corresponding author: rmrezaur@unimas.my*

INTRODUCTION

Rice husk (RH) is primarily composed of organic matter (75% to 90%), which includes lignin and cellulose, with inorganic matter accounting for the remaining 10% to 25% (Abbas *et al*. 2024). The RH's chemical makeup - namely cellulose, hemicellulose, lignin, and microscopic silica bodies, make RH suitable to be used in various applications including environmental remediation and chemical adsorption (Barbhuiya *et al.* 2025; Mesa *et al.* 2025). It is also estimated that RH contains a maximum of 25% of silica, with its average contents typically ranging between 10% to 20% (Barbhuiya *et al.* 2025; Park *et al.* 2023). Subsequently, rice husk ash (RHA) that is rich in amorphous state silica, is produced through combustion or thermal treatment of RH (Barbhuiya *et al.* 2025). Approximately 85% to 95% amorphous silica is obtained after complete combustion of RH (Abbas *et al.* 2024). The silica derived from rice husks can be utilized as an inexpensive precursor for Si-based materials or high-value-added silica particles (Park *et al.* 2023). Despite the commercial abundance of synthetic silica, the silica derived from plants, such as RH, offers notable advantages compared to those produced from minerals and synthetic origins. For instance, the processing steps are comparatively simple and do not require the usage of complex infrastructure or costly reagents, unlike in synthetic processes. Moreover, compared to other types of agricultural waste, the silica content in RH is also higher, which allows for direct and indirect applications in various fields (Oboh *et al.* 2023).

Rice is a staple, essential food for almost half of the world's population, including in Malaysia. After oil palm and rubber, rice is the third most significant crop (Dorairaj and Govender 2023). Sarawak is the fifth-largest rice-producing state in the country, with 134,260 hectares of land (Clifton *et al.* 2024). Millions of tons of RH are produced annually as a result of an average 526 million tons of annual global rice production (Tharaka *et al.* 2025). The husk generated during the rice processing is either burned or dumped as waste in most of the rice-producing countries (Hafez 2020). Currently, Malaysia mainly relies on traditional waste management methods that often harm the environment, with open burning commonly used for the disposal of agricultural waste. Although this method is effective to clear the fields and is low in cost, it emits a significant amount of harmful gases, such as carbon dioxide, methane, and particulates matter, into the atmosphere, contributing to air pollution (Harun *et al.* 2025).

The efficient usage of RH is therefore crucial to prevent environmental pollution. RHA, which is produced after the burning of RH, is detrimental to the nation's economy and environment. Apart from causing air pollution, it also damages the land where it is disposed of, including the surrounding area. It is critical for Malaysia to implement sustainable waste disposal techniques, given the substantial amounts of agricultural waste generated annually, and the environmental impact that comes with current existing practices. Henceforth, it is necessary to have a long-term rice husk waste management method to overcome those issues, and proper management of both RH and RHA is necessary. Consequently, RH has become popular as a value-added material for industrial and domestic processing (Hafez 2020; Harun *et al.* 2025; Tharaka *et al.* 2025).

To overcome the environmental issues caused by RH waste, the focus shifts to extracting silica from RH. The most applicable method to extract silica is through leaching treatment (Zarib *et al.* 2019). High purity silica can be produced from rice husk when acid leaching methods are used in the fabrication process. Acid leaching is the most effective method for removing metal impurities in comparison to the other methods. Additionally, *via* this leaching method, the silica's purity and surface area can be increased, resulting in high-quality silica (Yusof and Abu Bakar 2025). The extraction of the silica material is performed using inorganic acid, such as hydrochloric acid (HCl), solution for the leaching process (Zarib *et al.* 2019). HCl is shown to be more effective compared to other acid solutions for leaching process. Numerous studies have shown that HCl is the most effective leaching agent to obtain high purity amorphous silica (Kwan and Wong 2020).

While the extraction of silica through HCl leaching is well-documented, existing studies have focused on standardized commercial husks or different geographic regions. At the moment, there is a lack of data regarding the mineral profile as well as the valorization potential of RH originating from Roban, Sarawak. This study addresses this gap by characterizing the unique properties of this local biomass through chemical and thermal processes to achieve high whiteness and amorphous stability of silica.

The primary objective of this study is to systematically valorize RH sourced from Roban, Sarawak, by synthesizing amorphous silica with enhanced purity through HCl leaching. This research specifically aims to evaluate the impact of acid treatment to eliminate localized metallic impurities, and also to establish a definitive correlation between the chemical purification and the obtained physicochemical properties of the silica to meet the industrial standards for high-grade amorphous silica production.

EXPERIMENTAL

Materials

The rice husk was collected from a small rice mill located in Daerah Kecil Roban, Sarawak, Malaysia. The hydrochloric acid for the leaching process (HCl, 36.7 to 38.0%) was obtained from J.T. Baker (Phillipsburg, NJ, USA). The 10 wt% HCl solution was prepared from the standard stock of average concentration of 37 wt%. A total of 270 mL of the standard HCl stock were added into 730 mL of ultrapure water, producing 1 L of 10 wt% HCl solution.

Ultrapure water (Type I water) from the Arium Pro UV Ultrapure water system (Sartorius) was used throughout the experiment, from washing the RH until rinsing the acid-leached RHS for neutralization process. The sample was washed and rinsed using ultrapure water to clean the final product. Ultrapure water was used throughout the experiment because standard water (*e.g.* Type III water) contains trace minerals which could interfere with the analyses.

Synthesis of Rice Husk Silica (RHS) Particles

The raw RH was placed in 1000 mL beakers and washed 3 times by immersion in ultrapure water until fully submerged. The mixture was stirred manually to ensure thorough contaminant removal, and the entire process was conducted at room temperature (25 ± 2 °C). After that, the washed rice husk was dried in the oven (Memmert Universal Oven) at 100 °C for 16 h to ensure the husks were in a moisture-free state (Muralli *et al.* 2025).

The washed RH was placed in 3 medium sized alumina crucibles, and it was then placed inside an electric muffle furnace at 600 °C for 2 h. The obtained ashes (RHA) were further sieved using a 90 µm-size mesh screen. A total of 45 mL of 10% HCl are prepared, and 3 g of RHA were added to the solution. The 10 wt% HCl concentration was selected as it has been reported to be effective concentration to remove metallic impurities without causing significant silica dissolution. The RHA-HCl mixture was stirred at 200 rpm using a magnetic stirrer at room temperature (25 ± 2°C) for 2 h to ensure uniform contact and effective metal ion removal (Sankar *et al.* 2016). The obtained products were known as leached RHAs (LRHAs). The LRHAs were filtered using a vacuum filtration assembly equipped with polypropylene Buchner funnel to separate the HCl solution from the solid leached ashes. The LRHAs was subsequently washed with ultrapure water through repeated cycles of vacuum filtration until the filtrate reached a neutral value (pH ~7.0) before being dried inside oven at 150 °C for 24 h. The dried powder was then transferred to several alumina crucibles to ensure equal heating of the RHA. The crucible was then placed inside the electric muffle furnace with temperature 700 °C for 2 ½ h. Both calcinations temperature and duration were determined through preliminary test run.

Finally, white colored silica (SiO_2) powder was obtained. The obtained product is denoted as acid-leached RHS. Meanwhile, for the un-leached RHS, the process was similar, just without the acid treatment.

$$Yield\ (wt\%) = \frac{The\ amount\ of\ silica\ obtained\ (g)}{The\ amount\ of\ rice\ husk\ ash\ (g)} \times 100\% \quad (1)$$

Equation 1 was used to calculate the yield of silica obtained (by weight percentage) from both un-leached and acid-leached samples. The silica samples were then tested with X-ray diffraction (XRD) and Fourier transform infrared (FTIR) to check for the amorphousness of silica obtained and the type of groups band that existed in the particles, respectively (Yusof and Abu Bakar 2025).

Characterization of the RHS Particles

The color analysis for all the samples was performed by manually taking images of the samples, and to ensure consistency, all images were captured in a light-controlled environment with a fixed camera-to-sample distance and similar camera settings. Then, the images are processed using the 'Get Average Color of Image' web-based tool, developed by MatKL. The average color of the sample images in term of RGB was obtained. After that, the conversion of the RGB values into CIE-$L^*a^*b^*$ values was done using an RGB-to-Lab converter. The sample's luminosity is measured by the parameter "L^*", which ranges from black ($L^* = 0$) to white ($L^* = 100$). Meanwhile, the measurement range for the parameters "a^*" and "b^*" is -60 to +60. The parameter "a^*" represents the degree of measurement from green to red, while "b^*" is the degree of measurement from blue to yellow. The formula used to measure the whiteness index (WI) are shown in Eq. 2 (Mustafa Kamal *et al.* 2017):

$$WI = 100 - \sqrt{(100 - L^*)^2 + a^{*2} + b^{*2}} \quad (2)$$

The morphology of the samples was studied using field emission-scanning electron microscopy (FESEM). Prior to the morphological study, all samples were coated using gold/palladium (Au/Pd) (Quorum SC7620 Mini Sputter Coater; Quorum Technologies Ltd., Laughton, UK) to avoid the charging effect as well as for clearer images (Zainal *et al.* 2018). The surface morphology and elemental composition were analyzed using a JEOL JSM-IT500HR FESEM equipped with an integrated Energy Dispersive X-ray (EDX) spectrometer (JEOL Ltd., Akishima, Tokyo, Japan). The EDX analysis was performed to quantify the elemental composition of the samples at their surface (Gun *et al.* 2022).

For particle size distribution, SPAN is a measurement of size distribution, which mathematically describes the variation of sizes of particles in a powder sample. Equation 3 was used to define the SPAN of a volume-based size distribution (Li *et al.* 2022):

$$SPAN = \frac{D90 - D10}{D50} \quad (3)$$

Granulometric analysis of the powder particles, which obtained the values D_{10}, D_{50}, and D_{90} of the samples, as well as the samples' mean diameter was measured using the particle size analyzer (CILAS 1090; Cilas, Orléans, France). The equipment uses laser diffraction-based on Mie and Fraunhofer scattering theories in wavelength range of 635 and 830 nm. Samples were dispersed in ultrapure water and subjected to 60 seconds of internal ultrasonication within the CILAS 1090 unit to break up the agglomerates prior to laser diffraction measurement.

The samples underwent X-ray diffraction spectroscopy (XRD) analysis, with scanning 2θ ranging from 3° to 90° at step size of 0.01°/min. The XRD was utilized to check the state of silica amorphousness for all samples. A Rigaku Miniflex 600-C (Rigaku Corp., Tokyo, Japan) diffractometer was used to record and analyses the samples. Meanwhile, the functional groups of the samples were identified using Fourier transform infrared (FTIR) spectroscopy (Shimadzu IRAffinity -1; Shimadzu Corp., Kyoto, Japan), with each sample being analyzed using the ATR method in the 400 to 4000 cm^{-1} regions with the resolution of 1 cm^{-1}.

It should be noted that the reported values in the Results and Discussion sections were derived from a single optimized experimental run, conducted following the systematic refinement of all operational parameters to ensure maximum yield and purity of synthesized materials.

RESULTS AND DISCUSSION

Analysis of Visual Observations and Whiteness Index (WI)

Based on Fig. 1, the un-leached RHS was grey in color, while the acid-leached RHS was white. The difference in color can be attributed to the remaining impurities in the sample. Therefore, it can be suggested that HCl is an effective acid to leach impurities from RHAs. The metal content and organic compounds in the RHAs are successfully removed during the calcination process, which results in white-colored RHS (Wardhani *et al.* 2017). Amorphous silica are obtained when the calcination temperature is between 600 and 800 °C (Abbas *et al.* 2024). Furthermore, the acid treatment worked well in eliminating the majority of the carbonaceous and metallic impurities, thus producing completely white silica (Azat *et al.* 2019). Silica with enhanced purity is produced in solid phase through the acid leaching process, which dissolves metallic impurities in the strong acid solution (Park *et al.* 2023). The organic compounds in RH are reduced through heat treatment. Meanwhile, the acid chemical treatment is specifically used to eliminate inorganic contaminants or trace metals by converting them into soluble ions that are then filtered out. Ultimately, this process yields a white powder that is rich in silica. This finding is further supported by Singh *et al.* (2008), Kalapathy *et al.* (2003), and Yalçin and Sevinç (2001). According to the findings, this approach ensures that RHA is an excellent source material to produce pure amorphous silica (Hincapié-Rojas *et al.* 2018).

The visual transition from grey (un-leached) to white (acid-leached) provides immediate qualitative evidence of purification. This is further supported by the corresponding Whiteness Index (WI) values; however, these quantitative indices are treated as relative measurements to assess the efficiency of impurity removal under standardized experimental conditions. Furthermore, Table 1 shows the measured whiteness index (WI) of the samples. This measurement helped to show that acid leaching treatment significantly affecting the quality of ash, which includes color (Risfaheri *et al.* 2026). High positive WI index values indicate higher whiteness values for the specimen, whereas low (or even negative) values indicate lower whiteness values (Pérez *et al.* 2016).

The acid-leached RHS had the highest WI and L value, followed by the un-leached RHS, raw RH, and RHA, respectively. This sequence was consistent with the visual observation. Thus, it was shown that the combination of acid treatment (leaching of RHA using HCl) and heat treatment (calcination using muffle furnace) successfully produced white-colored silica. As for the redness, the RH had the highest "$a*$" value, resulting in a "redder" appearance, while the lowest "$a*$" value was RHA, which indicated a "greener" color. In terms of yellowness, RH also had the highest "$b*$" value, followed by the un-leached RHS, acid-leached RHS, and RHA, respectively (Milovanovic *et al.* 2020).

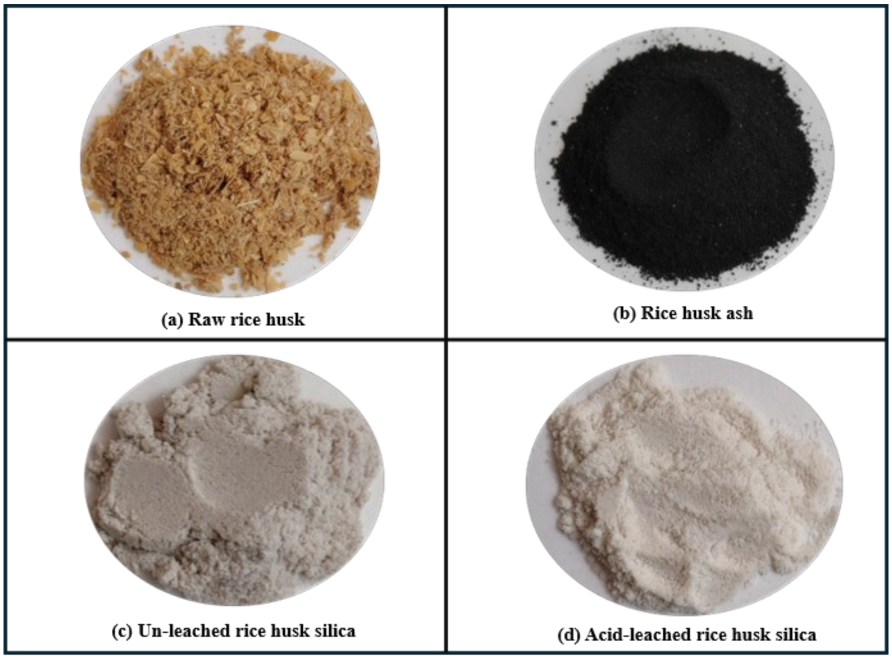

Fig. 1. Visual comparison of materials: (a) Raw RH, (b) RHA, (c) Un-leached RHS, and (d) Acid-leached RHS

Table 1. WI and CIE-*L*a*b** Color Parameters for RH, RHA, Acid-leached RHS, and Un-leached RHS

Sample	Values						
	R	*G*	*B*	*L**	*a**	*b**	WI
RH	170	134	100	58.52	9.09	23.55	51.45
RHA	51	50	49	20.85	0.21	0.79	20.85
Acid-leached RHS	177	166	162	74.58	2.29	1.38	74.44
Un-leached RHS	160	149	142	62.44	2.80	5.14	61.99

RHS Yield

The yields of RH to RHA as well as RHA to un-leached and acid-leached RHS are shown below:

$$Yield\ of\ RHA\ obtained\ (wt\%) = \frac{15.84\ g}{50.68\ g} \times 100\% = 31.25\ \%$$

$$Yield\ of\ un-leached\ RHS\ (wt\%) = \frac{0.76\ g}{1.76\ g} \times 100\% = 43.18\%$$

$$Yield\ of\ acid-leached\ RHS(wt\%) = \frac{0.68\ g}{1.76\ g} \times 100\% = 36.64\%$$

The above quantitative results demonstrate a clear effect of the purification process on the mass yield of the final silica product. The yield of the acid-leached RHS was calculated to be 36.64%, which was lower than the un-leached RHS at 43.18%. The reduction in the yield is regarded as a necessary and intended trade-off in achieving high purity silica. The observed reduction in yield (from 43.18% to 36.64%) is primarily attributed to the successful leaching of metallic impurities, as confirmed by the EDX data. However, this mass loss also reflects the cumulative effect of the partial dissolution of residual organic matter, the potential solubilization during the acid-soaking phase, and the unavoidable physical losses during the rigorous washing and filtration process required to achieve neutral pH. Acid leaching was very effective in eliminating or reducing impurities. HCl-leaching can dissolve inorganic metallic impurities, such as iron (Fe), sodium (Na), potassium (K), and magnesium (Mg), that are found in rice husk (Zainal *et al.* 2019; Yusof and Abu Bakar 2025).

This finding is strongly supported by the other characterization data, namely, the WI and EDX. The considerable WI value of the acid-leached RHS compared to the other samples provided visual evidence of the successful removal of colored impurities. Furthermore, the EDX analysis demonstrated that the acid leached process silica had enhanced purity compared to the un-leached one. In contrast with the un-leached RHS, which still showed traces of metallic impurities, such as Mg and K, whereas the acid-leached RHS was composed predominantly of C, Si, and O. This further confirms that the purification process through acid-leaching successfully reduced the impurity concentration. The purity of final silica product was thus maximized, consequently leading to the low mass yield value.

Morphological, Composition, and Surface Analyses

FESEM – SEM

The FESEM images of RH, RHA, un-leached RHS, and acid-leached RHS are presented in Fig. 2.

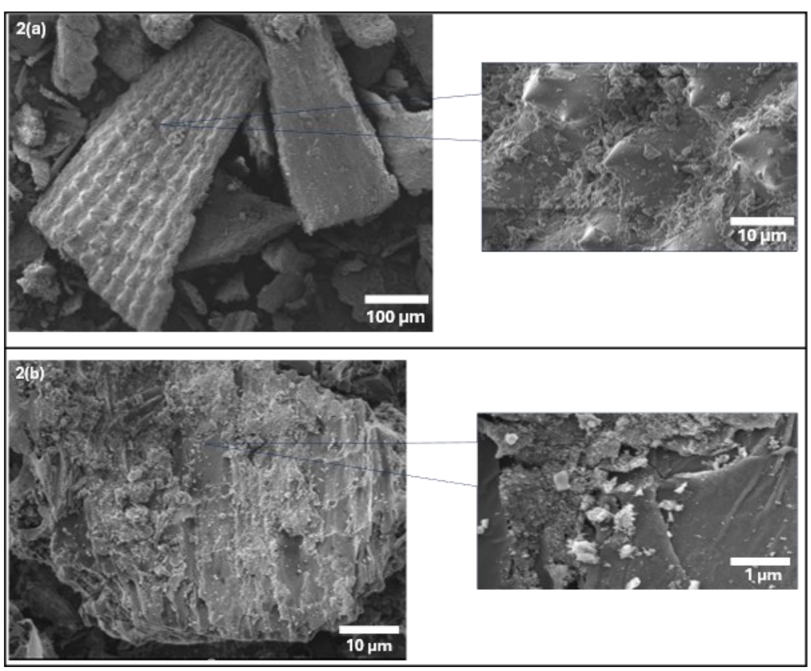

Fig. 2 a,b. FESEM images of (a) Raw rice husk, and (b) Rice husk ash

The micrographs demonstrate the thermal destruction of the rice husk's organic matter, hence resulting in the formation of a porous structure through amorphous carbonization (Baraitaru *et al.* 2019). Meanwhile, the silica dioxide (SiO_2) produced was found to have varying surface morphologies. The non-uniform formations indicate an amorphous phase in the produced silicon dioxide (Irzaman *et al.* 2020). The findings are in agreement with the XRD data in Fig. 4 (broad peak between 2θ = 20° and 25°).

Figures 2(a) and (b) show the FESEM images of RH and RHA. For the RH, the image is of the outer layer, namely the epidermis. From Fig. 2(a), it was observed that the morphology of the outer epidermis displayed ridge structures with furrows as well as conical protrusions. The micro-bumps' morphology with a tip-like structure on top can be observed in the highlighted area (Chen *et al.* 2017). It can be seen that the RH structure changed after the calcination at 600 °C, where the RHA (Fig. 2(b)) had wavy configuration on flat ground (Gun *et al.* 2022).

Figure 2 (c) and (d) correspond to the FESEM images of un-leached RHS and acid-leached RHS, respectively. From the figures, the FESEM micrographs of the acid-leached RHS reveal a more fragmented and accessible surface topography compared to the un-leached RHS. This finding is attributed to the combination of thermal and chemical treatment used to extract silica from the RHA. Leaching with strong acids, such as HCl, helps to increase the pores by removal of both inorganic impurities (*e.g.*, metallic impurities) and organic compounds such as hemicellulose, lignin, and cellulose (Wardhani *et al.* 2017; Zarib *et al.* 2019). While these qualitative observations suggest an increase in the surface accessibility, it is important to note that direct porosity metrics, such as BET surface area, were not measured in this study. Nonetheless, the observed morphological changes are consistent with the successful dissolution of the rigid epidermal layer. This is consistent with the EDX data obtained, where the acid-leached RHS had a higher SiO_2 content (97.26%) in comparison to the un-leached RHS (91.14%). Furthermore, the EDX also demonstrated that the acid-leached RHS was composed of only C, O, and Si elements, while the un-leached RHS still showed traces of metallic impurities, such as P, K, Ca, and Fe.

Additionally, it appeared that from Fig. 2(d) the agglomerated SiO_2 particles had a flake-like structure. These results are likely to be related to the selection of HCl as the leaching acid. HCl is a strong inorganic acid, which causes the powder to finely disperse and form agglomerates. Cellulose and hemicellulose break down easily during calcination, but lignin may retain inorganic impurities and unburned carbon residues. In order to overcome this matter, acid leaching is done, enabling the production of high-purity silica with large specific surface area through elimination of organic matter and metallic impurities. Acid leaching hydrolyses both hemicellulose and cellulose into lower molecular weight compounds by weaking their hydrogen bonds (Risfaheri *et al.* 2026). Additionally, strong inorganic acid such as HCl causes the RH powder to fine and form agglomerate. The particle sizes in the range of several microns are formed by the aggregation of smaller particles in the submicron range. The leaching process then causes the powders to stick together, forming agglomerates (Zarib *et al.* 2019).

According to the EDX analysis results shown in Table 2, which provides a semi-quantitative assessment of the sample surface, the SiO_2 content for both RHS samples contained is relatively high, regardless of being acid-treated or not. While EDX is a surface-localized technique and may not represent absolute bulk purity as precisely as XRF or ICP-OES, the substantial reduction in detectable metallic impurities (K, Ca, Fe) coupled with a significant increase in the WI. During the thermal treatment using an electric furnace, the original organic contents, such as hemicellulose, lignin, pentosanes, *etc.*, were successfully removed. However, metallic impurities were then produced in the RHA due to the direct burning in the electric furnace. Through utilizing strong acid, such as HCl, those metallic impurities were able to be eliminated (Dhaneswara *et al.* 2020). This suggests that the HCl leaching protocol effectively removes acid-soluble inorganic impurities, resulting in amorphous silica with enhanced purity. Apart from that, the higher silica content of the acid-leached RHS may be explained by the fact that it is possible that hydrolysis and structural deformation caused the organic framework to loosen, hence facilitating in the extraction of silica (Tharani and Ananthasubramanian 2024).

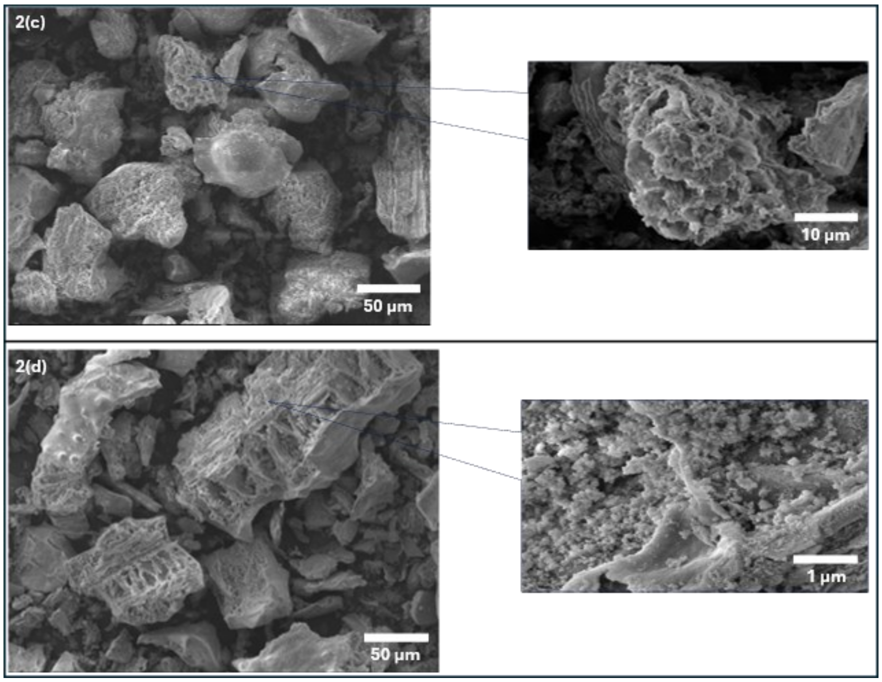

Fig. 2 c,d. FESEM images of (c) Un-leached Rice husk silica, and (d) Acid-leached rice husk silica

Table 2. Elemental Composition of Samples (wt%) *via* EDX Analysis

Sample		RH	RHA	Un-leached RHS	Acid-leached RHS
Element (wt%)	C	50.51	70.89	2.22	2.74
	O	35.98	22.74	48.73	57.63
	Si	3.44	4.59	42.41	39.63
	P	4.75	0.81	1.42	
	K	2.40	0.97	1.63	
	Ca	0.84		0.61	
	Fe			2.99	
	Mo	0.60			
	Mg	1.48			
Total (wt%)		100.00	100.00	100.00	100.00

Particle size distribution

Diameter is particularly important in defining uniform spherical size. Particle size has a substantial impact on the properties of particulate matter. As a result, it is frequently regarded as a critical measurement of its property and performance. The particle size distribution (PSD) is commonly described using *D*-values, *i.e.*, D_{10}, D_{50}, and D_{90}. $D_{[i]}$ represents the percentage of the total mass that is made up of smaller particles. The D_{10} indicates that 10% of the sample's mass has a diameter smaller than this value. The diameter of 50% of the distribution is implied to be below this value by the D_{50} (median), while 90% of the distribution is implied to be below this value by D_{90}. The formula SPAN= $(D_{90} - D_{10}) / D_{50}$ quantifies the Gauss distribution's width based on the metric calculation. SPAN measures particle stretches from 10% to 90% diameter relative to the normalized mid-value (Zegzulka *et al.* 2020; Haramkar *et al.* 2021; Konstanty and Tyrala 2024). A large SPAN value indicates a wider range of particle sizes in the powder. Meanwhile, lower SPAN values imply a narrower range of particle size, while a value of 0 suggests that the particle has monodisperse distribution (Moolchandani *et al.* 2014).

The data presented in Table 3 are obtained from a single, representative optimized run. From Table 3 and Fig. 3a, acid-leached RHS had the smallest mean diameter of 33.02 µm, followed by the un-leached RHS (33.63 µm), and the RHA had the largest mean diameter among the samples (45.27 µm). This outcome is in line with results from a study conducted by Mohd *et al.* in 2024, where RHA that was treated with HCl would result in small particle size as HCl has strong acidic strength, which influences the leaching process (Faiza Mohd *et al.* 2024). The result also showed that acid-leached RHS had the lowest SPAN value of 1.66, implying that compared to the other samples, the RHAs that were treated with acid produced silica with a narrow range of particle size.

Table 3. PSD (D_{10}, D_{50}, D_{90}) and SPAN Values for RHA, Un-leached RHS, and Acid-leached RHS

	RHA (µm)	Un-leached RHS (µm)	Acid-leached RHS (µm)
Mean Diameter	45.27	33.63	33.02
D_{10}	9.09	7.67	8.12
D_{50}	44.11	31.86	31.41
D_{90}	83.36	61.85	60.26
SPAN	1.68	1.70	1.66

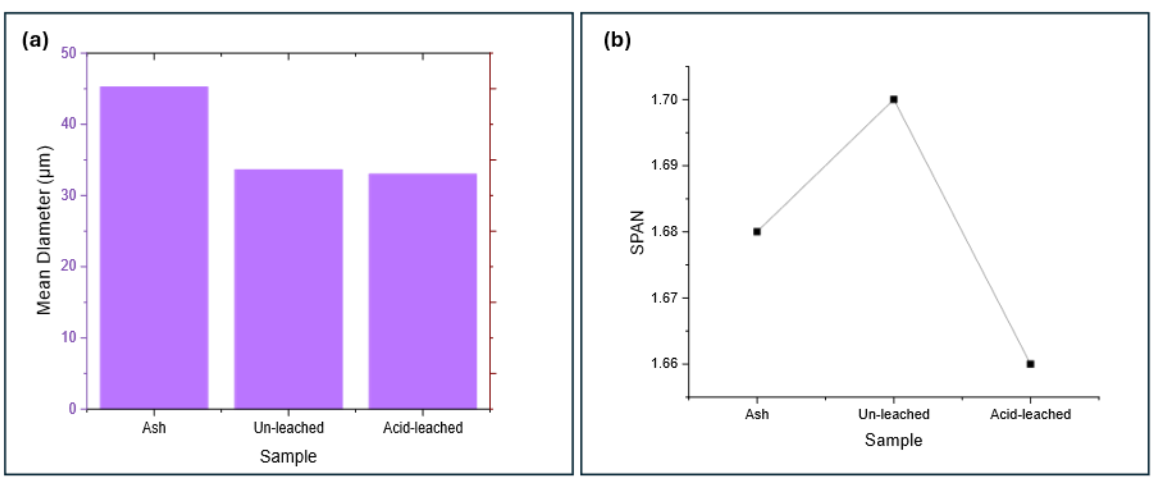

Fig. 3. Particle size distribution analysis: (a) mean diameter and (b) SPAN values; for RHA, Un-leached RHS, and Acid-leached RHS

XRD Analysis

Figure 4 displays the XRD patterns for RHA, un-leached RHS, and acid-leached RHS. The absence of sharp peaks in the XRD patterns verifies the presence of amorphous silica. Atoms are arranged at random in amorphous materials. Therefore, during the XRD scanning sequence, there is no crystal diffraction signal produced and recorded (Wong *et al.* 2019). As shown in Fig. 4, the broad humps or broadened, non-sharp peaks observed at the diffraction angle of 2θ = 20° to 25° indicate the amorphous phase of the silica (Khoshnood Motlagh *et al.* 2022; Kumalasari *et al.* 2024). This result was consistent with the data obtained in the FTIR (Fig. 5), where peaks at 790 to 800 cm^{-1} are attributed to the amorphous silica structure. This suggests that the combustion process helps to transform the crystalline cellulose structure into an amorphous, random, disordered structure that may be capable of adsorption (Soltani *et al.* 2014). Because both un-leached and acid-leached were found to be amorphous, the HCl treatment onto the samples did not affect the transformation of silica structure to the crystalline state (Abdullah *et al.* 2022).

It can be seen from Fig. 4 that, in all three samples, there were some minor peaks observed. These small peaks represent minor crystalline phases (Muralli *et al.* 2025) and are likely due to the residual carbon char ash in the particle (El-Sakhawy *et al.* 2022). However, in the acid-leached RHS sample, the intensity of those peaks is significantly reduced, indicating the successful dissolution and removal of majority of the crystalline inorganic impurities through HCl leaching. Furthermore, for RHA and un-leached RHS, the peaks might be due to traces of impurities in both samples. It was discovered that rice husk's potassium content is the primary cause of silica crystallization during the combustion process. Carbon is trapped in the melted portion of the silica due to the eutectic compounds of potassium and silica, hence preventing the carbon from escaping during heating. The trapped carbon would then cause the appearance of a black particle when the temperature increases. This demonstrates that the state of silica had changed from amorphous to crystalline. Alkali metals can be removed more effectively by using mineral acid, such as HCl, compared to organic acids (Abbas *et al.* 2024). The comparative reduction in these crystalline peaks serves as structural validation, confirming that acid-leached RHS has more refined amorphous silica network compared to its un-leached counterparts. This also accords with earlier findings in EDX, which showed that the acid-leached RHS has no impurities, while the other two samples (RHA and un-leached RHS) had traces of metallic impurities such as P, K, Ca, Fe, Mo, and Mg.

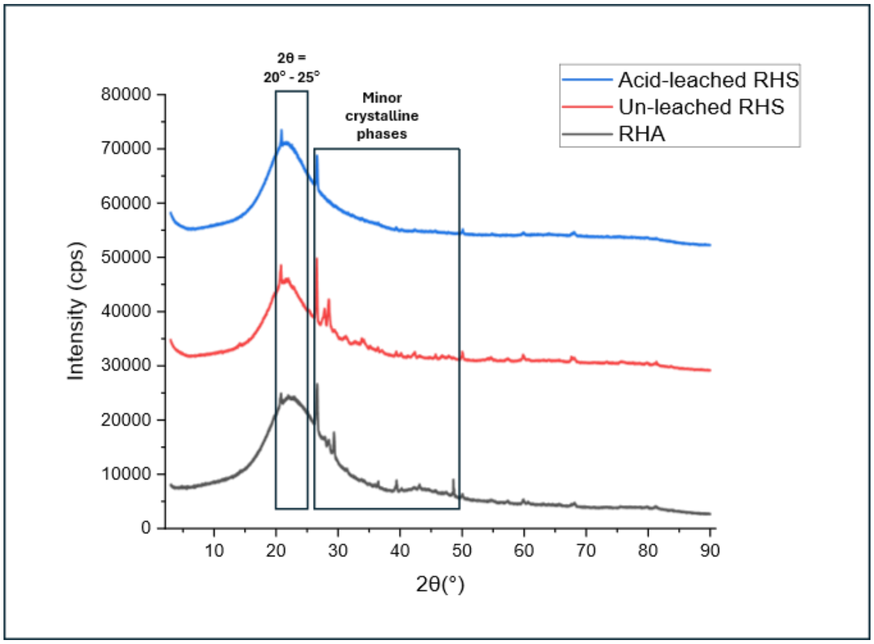

Fig. 4. XRD analysis of RHA, un-leached, and acid-leached RHS

FTIR Analysis

The FTIR analysis is used to identify the bio-silica bonding groups and Fig. 5 presents the results obtained from the infrared (IR) spectroscopy ranging from 400 to 4000 cm^{-1}. The main functional groups of amorphous silica are siloxane (Si-O-Si), silanol (Si-O-H), and Si-H bonds (Kumalasari *et al.* 2024). The changes in the silica surface structure, which are caused by the silica surface reaction with water, have an effect on the silica's interaction with other materials. Specifically, the atomic structure of the silica surface is affected by hydroxylation and development of a monolayer of adsorbed water. Thus, the adhesion energy is reduced. Under ambient conditions, the hydroxylated silica surface's silanol functional groups are affected by small molecules such as water (Hamidu *et al.* 2025).

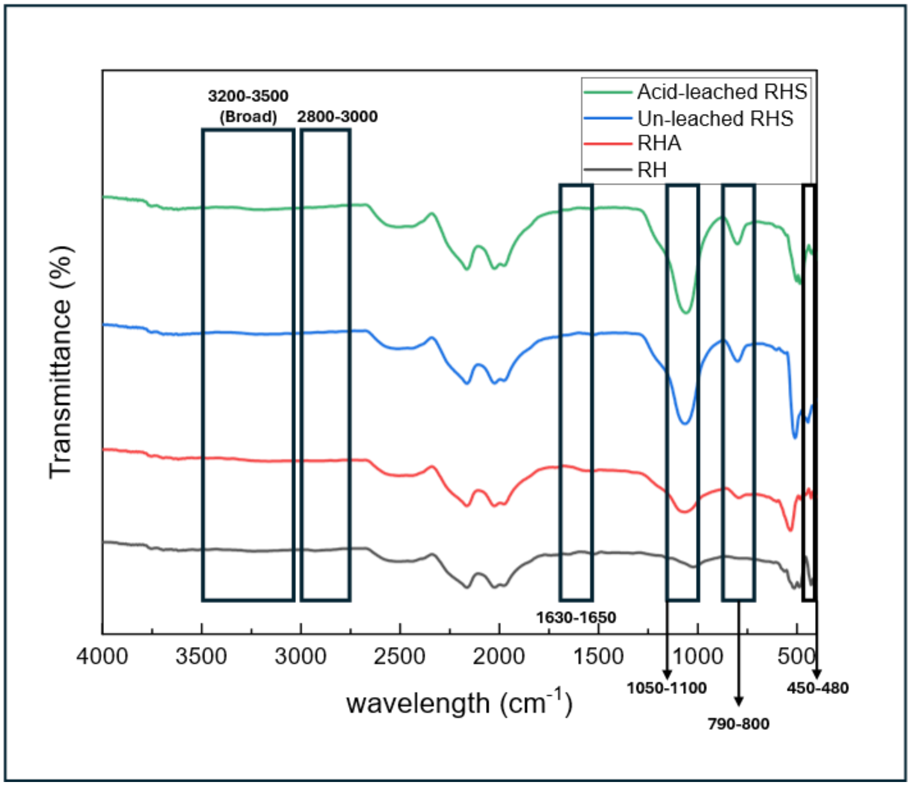

Fig. 5. FTIR analysis of RH, RHA, Un-leached RHS, and Acid-leached RHS

As shown in Fig. 5, the band at 470 cm^{-1} corresponds to the O-Si-O band bending vibration (Chik and Shaari 2022). This is further supported by few studies. For instance, the O-Si-O framework shows bending vibrations at peaks 459, 466, 467, and 469 cm^{-1} (Wardhani *et al.* 2017). Additionally, the 455.2 cm^{-1} band is attributed to Si-O-Si stretching and bending vibrations (Dhaneswara *et al.* 2020). The peaks in the spectra at wavenumber 700 to 800 cm^{-1} refer to the stretching symmetric bond of Si-O (silanol) (Azmi *et al.* 2016; Khoshnood Motlagh *et al.* 2022). Similarly, the stretching and asymmetrical stretching vibration of Si-O-amorphous SiO_2 and Si-O-Si can be ascribed to the IR spectra at ranges 778 to 799 cm^{-1} and 1035 to 1125 cm^{-1}, respectively (Haider *et al.* 2022; Lailiyah *et al.* 2024). These characteristics groups of amorphous silica demonstrate the presence of amorphous silica components in every sample (Yuan *et al.* 2024). The strong adsorption peaks that were detected at peaks 497 and 795 cm^{-1} corresponded to Si-O-Si bending and Si-O-Si symmetric stretching modes of vibration (Yuvakkumar *et al.* 2014).

From Fig. 5, it is apparent that all four samples' FTIR spectra showed a vibrational signature at 1050 to 1100 cm^{-1}, and the peaks became the most intense in the acid-leached RHS compared to the RH. Those peaks correspond to the asymmetric stretching and bending vibrations of Si-O-Si bonds, indicating the presence of siloxane structural bonding. According to the literature, SiO_2's adsorption band falls between 1000 and 1100 cm^{-1} (Azmi *et al.* 2016; Haider *et al.* 2022; Yuan *et al.* 2024). This is further verified in study by Kumalasari *et al.* (2024), where peaks at 1044 to 1100 cm^{-1} are attributed to the asymmetric siloxane bond, and a study by Gun *et al.* (2022) also reflects the same result. The spectra ranging from 1200 to 1000 cm^{-1} were due to the vibration's superposition of the C-OH bond and Si-O bond in the siloxane groups. From the FTIR data, the acid-leached RHS had higher absorbance compared to the un-leached, RHA, and RH despite having similar absorbance in the symmetric siloxane region. This finding provides evidence that the acid treatment clearly affected the asymmetric siloxane network in silica, as the high absorbance is due to the removal of acid-soluble impurities (Haider *et al.* 2022).

However, the band existing around 1620 cm^{-1} could be due to the O-H stretching of adsorbed water or C=C vibration (Dhaneswara *et al.* 2019). Likewise, the band occurring at 1633 cm^{-1} also corresponds to carbonyl (C=O) groups (Gun *et al.* 2022). The adsorption bands at peak 3445.0 and 1625.8 cm^{-1} are attributed to the adsorbed water's H-O-H stretching and bending modes on the surface of SiO_2, respectively (Faizul *et al.* 2013; Lailiyah *et al.* 2024).

The symmetric and asymmetric stretching vibrations of aliphatic C-H bonds associated with $-CH_3$ and CH_2 groups in hemicellulose, cellulose, and lignin, are demonstrated by the peak at 2921 cm^{-1} (Azat *et al.* 2019). Notably, the CH_2 stretch vibrations could also be present due to residual carbon ashes (El-Sakhawy *et al.* 2022). The peak existing around 2917 cm^{-1} is attributed to the C-H stretching and bending modes (Khoshnood Motlagh *et al.* 2022).

Finally, a broad band was shown at 3440 to 3455 cm^{-1}, which refers to the bonding surface silanol groups (Si-OH) asymmetric stretching vibrations (El-Sakhawy *et al.* 2022). Additionally, the vibrational peaks that occurred around 3400 cm^{-1} are assigned to chemically bound water, which is represented by O-H and H-O-H bonds (Yuan *et al.* 2024).

CONCLUSIONS

1. The combination of thermal calcination and HCl leaching was highly effective for producing amorphous silica with enhanced purity from rice husk, achieving a silica with SiO_2 content of 97.26 wt%.
2. Acid leaching successfully eliminated most of the colored carbonaceous and metallic impurities (P, K, Ca, and Fe), resulting in a notable improvement in the whiteness index and a transition from greying appearance to pure white.
3. The observed reduction of the mass yield from 43.18% (un-leached) to 36.64% (acid-leached) was mainly ascribed to the removal of the metallic impurities through HCl treatment, but it was also a result of combination of factors such as partial dissolution of residual organic matter, the potential solubilization during the acid-soaking phase, and the unavoidable physical losses during the rigorous washing and filtration process required to achieve neutral pH.
4. FESEM micrographs of the acid-leached RHS revealed a more fragmented and accessible surface topography compared to the un-leached RHS.
5. Chemical treatment refined the physical properties of the silica, producing a narrower particle size distribution (SPAN value of 1.66) and a reduced mean particle diameter of 33.02 µm, in comparison to its un-leached counterparts.
6. Both XRD and FTIR analyses confirmed that the structural integrity of the material is maintained throughout the process, with both un-leached and acid-leached samples retaining a predominantly amorphous state.

ACKNOWLEDGMENTS

This Project was funded by the Deanship of Scientific Research (DSR) at King Abdulaziz University, Jeddah, Saudi Arabia under grant no. (IPP: 254-130-2025). The authors, therefore, acknowledge with thanks DSR for technical and financial support.

Conflict of Interest

The authors declare that they have no known competing financial interests or personal relationships that could have appeared to influence the work reported in this paper.

Use of Generative AI

The authors used Quillbot for paraphrasing and refining the clarity of the manuscript. Additionally, Gemini (Google) was employed to assist with data analysis and as a grammar as well as word structure checker to ensure academic rigor. The authors take full responsibility for the final content and integrity of the work. No generative AI was used in the preparation of images, figures, graphs, or diagrams.

REFERENCE CITED

Abbas, M. A., Kwan, W. H., Samsudin, M. H., and Hai, T. K. (2024). "Optimising factors for the production of amorphous rice husk ash *via* combustion process for sustainable construction: A review," *Journal of Advanced Research in Applied Mechanics* 120(1), 50-61. https://doi.org/10.37934/aram.120.1.5061

Abdullah, M. N., Mustapha, F., Ahmad, K. A., Mustapha, M., Khan, T., Singh, B., and Sebaey, T. A. (2022). "Effect of different pre-treatment on the microstructure and intumescent properties of rice husk ash-based geopolymer hybrid coating," *Polymers* 14(11), article 2252. https://doi.org/10.3390/polym14112252

Azat, S., Sartova, Z., Bekseitova, K., and Askaruly, K. (2019). "Extraction of high-purity silica from rice husk *via* hydrochloric acid leaching treatment," *Turkish Journal of Chemistry* 43(5), 1258-1269. https://doi.org/10.3906/kim-1903-53

Azmi, M. A., Ismail, N. A. A., Rizamarhaiza, M., Hasif, A. A. K. W. M., and Taib, H. (2016). "Characterisation of silica derived from rice husk (Muar, Johor, Malaysia) decomposition at different temperatures," *AIP Conference Proceedings* 1756(1), article 020005. https://doi.org/10.1063/1.4958748

Baraitaru, A., Deák, G., Boboc, M., Olteanu, M., Matei, M., Lumînaroiu, L., and Raischi, M. (2019). "Synthesis of rice husk ash through various methods and determination of the highest silicon content for subsequent applications," *AIP Conference Proceedings* 2129(1), article 020093. https://doi.org/10.1063/1.5118101

Barbhuiya, S., Das, B. B., Adak, D., Rajput, A., and Katare, V. (2025). "Rice husk ash in structural concrete: Influence on strength, durability and sustainability," *Discover Concrete and Cement* 1, article 14. https://doi.org/10.1007/s44416-025-00013-9

Chen, Z., Xu, Y., and Shivkumar, S. (2017). "Microstructure and tensile properties of various varieties of rice husk," *Journal of the Science of Food and Agriculture* 98(3), 1061-1070. https://doi.org/10.1002/jsfa.8556

Chik, N. S. I., and Shaari, N. Z. K. (2022). "Effect of rice husk ash gel on the properties of integral membrane from a blend of polysulfone/ chitosan/ polyvinyl alcohol," *AIP Conference Proceedings* 2610(1), article 020010. https://doi.org/10.1063/5.0099563

Clifton, Z. F., Yeo, F. K. S., Embuas, R. P. T. S., Kalu, M., Shabdin, Z., and Lai, L. S. (2024). "Preliminary characterisation of lowland and upland rice from Sarawak, Malaysian Borneo," *Borneo Journal of Resource Science and Technology* 14(1), 123-138. https://doi.org/10.33736/bjrst.5653.2024

Dhaneswara, D., Fajar Fatriansyah, J., Kusuma Wardana, A., Nurul Haqoh, A., and Aida Khairunnisa, S. (2019). "The study of thermal decomposition of rice husk in silica production: The effect of hydrochloric acid leaching," *IOP Conference Series: Materials Science and Engineering* 547(1), article 012032. https://doi.org/10.1088/1757-899X/547/1/012032

Dhaneswara, D., Fatriansyah, J. F., Situmorang, F. W., and Haqoh, A. N. (2020). "Synthesis of amorphous silica from rice husk ash: Comparing HCl and CH_3COOH acidification methods and various alkaline concentrations," *International Journal of Technology* 11(1), 200-208. https://doi.org/10.14716/ijtech.v11i1.3335

Dorairaj, D., and Govender, N. T. (2023). "Rice and paddy industry in Malaysia: Governance and policies, research trends, technology adoption and resilience," *Frontiers in Sustainable Food Systems* 7, article 1093605. https://doi.org/10.3389/fsufs.2023.1093605

El-Sakhawy, M., Adel, A. M., Diab, M. A., and Al-Shemy, M. (2022). "Facile methods for the preparation of micro- and mesoporous amorphous silica from rice husk," *Biomass Conversion and Biorefinery* 12(10), 4709-4718. https://doi.org/10.1007/s13399-020-01112-2

Faiza Mohd, A., Mohamad Shokri, A. H., and Ibrahim, N. (2024). "The effect of chemical treatment on rice husk ash silica-filled natural rubber vulcanisates," *Malaysian Journal of Chemistry* 26(3), 302-311. https://doi.org/10.55373/mjchem.v26i3.302

Faizul, C. P., Abdullah, C., and Fazlul, B. (2013). "Extraction of silica from palm ash using citric acid leaching treatment: Preliminary result," *Advanced Materials Research* 795, 701-706. https://doi.org/10.4028/www.scientific.net/AMR.795.701

Gun, M., Arslan, H., Saleh, M., Yalvac, M., and Dizge, N. (2022). "Optimization of silica extraction from rice husk using response surface methodology and adsorption of safranin dye," *International Journal of Environmental Research* 16, article 20. https://doi.org/10.1007/s41742-022-00399-5

Hafez, A. I. (2020). "Synthesis of silica and silica compounds based on rice husk ash: Article review," *Water, Energy, Food and Environment* 1(2), 37-45. https://doi.org/10.18576/wefej/010204

Haider, J. B., Haque, M. I., Hoque, M., Hossen, M. M., Mottakin, M., Khaleque, M. A., Johir, M. A. H., Zhou, J. L., Ahmed, M. B., and Zargar, M. (2022). "Efficient extraction of silica from openly burned rice husk ash as adsorbent for dye removal," *Journal of Cleaner Production* 380(Part 2), article 135121. https://doi.org/10.1016/j.jclepro.2022.135121

Hamidu, I., Afotey, B., Kwakye-Awuah, B., and Anang, D. A. (2025). "Synthesis of silica and silicon from rice husk feedstock: A review," *Heliyon* 11(4), article e42491. https://doi.org/10.1016/j.heliyon.2025.e42491

Haramkar, S. S., Thombre, G. N., Jadhav, S. V., and Thorat, B. N. (2021). "The influence of particle(s) size, shape and distribution on cake filtration mechanics-a short review," *Comptes Rendus Chimie* 24(2), 255-265. https://doi.org/10.5802/CRCHIM.84

Harun, S. N., Alias, A., and Siregar, K. (2025). "Toward a sustainable energy future:

Agricultural waste as a bioenergy resource in Malaysia," *Journal of Climate Change and Space Science* 1(1), article 3. https://doi.org/10.17576/jccass.0101.2025.03

Hincapié-Rojas, D. F., Rosales-Rivera, A., and Pineda-Gomez, P. (2018). "Synthesis and characterisation of submicron silica particles from rice husk," *Green Materials* 6(1), 15-22. https://doi.org/10.1680/jgrma.17.00019

Irzaman, Cahyani, I. D., Aminullah, Maddu, A., Yuliarto, B., and Siregar, U. J. (2020). "Biosilica properties from rice husk using various HCl concentrations and frequency sources," *Egyptian Journal of Chemistry* 63(2), 363-371. https://doi.org/10.21608/ejchem.2019.8044.1679

Khoshnood Motlagh, E., Asasian-Kolur, N., and Sharifian, S. (2022). "A comparative study on rice husk and rice straw as bioresources for production of carbonaceous adsorbent and silica," *Biomass Conversion and Biorefinery* 12(12), 5729-5738. https://doi.org/10.1007/s13399-020-01145-7

Konstanty, J., and Tyrala, D. (2024). "Particle sizing and surface area measurements: A comparative assessment of commercial air permeability and laser light diffraction instruments," *Applied Sciences (Switzerland)* 14(11), article 4802. https://doi.org/10.3390/app14114802

Kumalasari, M. R., Beladona, S. U. M., Gracia, A. N., Sugiyani, T., Wulandari, O. R., Imelya, M., Syaima, H., and Hanif, Q. A. (2024). "Rice husk ash: A promising heavy metal adsorbent for wastewater treatment," *Walisongo Journal of Chemistry* 7(1), 26-36. https://doi.org/10.21580/wjc.v7i1.18852

Kwan, W. H., and Wong, Y. S. (2020). "Acid leached rice husk ash (ARHA) in concrete: A review," *Materials Science for Energy Technologies* 3, 501-507. https://doi.org/10.1016/j.mset.2020.05.001

Lailiyah, Q., Darmayanti, N. T. E., Mulyana, M. R., Nuryatini, N., Hapiddin, A., Basuki, B., Zuas, O., Rahmah, S. A., Fadhila, A. N., Aryana, N., *et al.* (2024). "Amorphous silica microsphere from openly burned rice husk ash as an efficient adsorbent for ultrasound-assisted methylene blue removal," *Rasayan Journal of Chemistry* 17(1), 95-104. https://doi.org/10.31788/RJC.2024.1718726

Li, W., Wang, J., Zhou, Y., Shao, Y., Zhang, H., and Zhu, J. (2022). "An investigation into the effect of particle size distribution on the fluidization behavior of Group C and Group A particles," *Powder Technology* 398, article 117142. https://doi.org/10.1016/j.powtec.2022.117142

Mesa, S., Castro-Ladino, J. R., Amaya, S. L., Manrique, C., Echavarría, A., Hoyos-Ayala, D. A., and Uran, L. (2025). "Comprehensive characterization of carbonaceous material derived from rice husk pyrolysis and its potential for CO_2 adsorption," *Materials* 18(22), 1-16. https://doi.org/10.3390/ma18225151

Milovanovic, B., Djekic, I., Miocinovic, J., Djordjevic, V., Lorenzo, J. M., Barba, F. J., Mörlein, D., and Tomasevic, I. (2020). "What is the color of milk and dairy products and how is it measured?," *Foods* 9(11), article 1629. https://doi.org/10.3390/foods9111629

Moolchandani, V., Augsburger, L. L., Gupta, A., Khan, M., Langridge, J., and Hoag, S. W. (2014). "Characterization and selection of suitable grades of lactose as functional fillers for capsule filling: Part 1," *Drug Development and Industrial Pharmacy* 41(9), 1452-1463. https://doi.org/10.3109/03639045.2014.957703

Muralli, A., Kwan, W. H., Abbas, M. A., and Samsudin, M. H. (2025). "Characterizations of rice husk based silica made from acid leaching extraction method," *E3S Web of Conferences* 603, article 02004.

https://doi.org/10.1051/e3sconf/202560302004

Mustafa Kamal, M., Baini, R., Mohamaddan, S., Selaman, O. S., Ahmad Zauzi, N., Rahman, M. R., Abdul Rahman, N., Chong, K. H., Atan, M. F., Abdul Samat, N. A. S., *et al.* (2017). "Effect of temperature to the properties of sago starch," *IOP Conference Series: Materials Science and Engineering* 206(1), article 012039. https://doi.org/10.1088/1757-899X/206/1/012039

Oboh, I. O., Ihom, A. P., and Markson, I. E. (2023). "Use of rice husk and rice husk ash for metallurgical grade silicon: The production, purification and upgrade," *International Journal of Engineering and Modern Technology* 9(1), 83-99. https://doi.org/10.56201/ijemt.v9.no1.2023.pg83.99

Park, J. Y., Gu, Y. M., Chun, J., Sang, B. I., and Lee, J. H. (2023). "Pilot-scale continuous biogenic silica extraction from rice husk by one-pot alkali hydrothermal treatment and ball milling," *Chemical and Biological Technologies in Agriculture* 10, article 102. https://doi.org/10.1186/s40538-023-00479-4

Pérez, M. D. M., Ghinea, R., Rivas, M. J., Yebra, A., Ionescu, A. M., Paravina, R. D., and Herrera, L. J. (2016). "Development of a customized whiteness index for dentistry based on CIELAB color space," *Dental Materials* 32(3), 461-467. https://doi.org/10.1016/j.dental.2015.12.008

Risfaheri, Hidayat, T., Yuliani, S., Hoerudin, Wahyuningsih, K., Yulianto, A., Setyawan, N., Winarti, C., and Arif, A. Bin. (2026). "Sustainable production of high-purity amorphous silica from rice husk: A comparative study on the impact of fresh and reused hydrochloric acid leaching," *South African Journal of Chemical Engineering* 56(February), article 100848. https://doi.org/10.1016/j.sajce.2026.100848

Sankar, S., Sharma, S. K., Kaur, N., Lee, B., Kim, D. Y., Lee, S., and Jung, H. (2016). "Biogenerated silica nanoparticles synthesized from sticky, red, and brown rice husk ashes by a chemical method," *Ceramics International* 42(4), 4875-4885. https://doi.org/10.1016/j.ceramint.2015.11.172

Soltani, N., Bahrami, A., Pech-Canul, M. I., and González, L. A. (2014). "Review on the physicochemical treatments of rice husk for production of advanced materials," *Chemical Engineering Journal* 264, 899-935. https://doi.org/10.1016/j.cej.2014.11.056

Tharaka, D. N., Tissera, N. D., Priyadarshana, G., and Dahanayake, D. (2025). "A comprehensive review of hierarchical porous carbon synthesis from rice husk," *Rice Science* 32(4), 499-511. https://doi.org/10.1016/j.rsci.2025.04.009

Tharani, D., and Ananthasubramanian, M. (2024). "Influence of pre-treatment processes on the purity and characteristics of silica extracted from rice husk," *Biomass Conversion and Biorefinery* 14(11), 12517-12529. https://doi.org/10.1007/s13399-022-03728-y

Wardhani, G. A. P. K., Nurlela, N., and Azizah, M. (2017). "Silica content and structure from corncob ash with various acid treatment (HCl, HBr, and citric acid)," *Molekul* 12(2), 174-181. https://doi.org/10.20884/1.jm.2017.12.2.382

Wong, Y. S., Kwan, W. H., Lee, F. K., Sin, J. C., and Wai, S. H. (2019). "Performance of acid leached rice husk ash (ARHA) in Mortar," *International Journal of Integrated Engineering* 11(9), 285-294. https://doi.org/10.30880/ijie.2019.11.09.030

Yuan, S., Hou, Y., Liu, S., and Ma, Y. (2024). "A comparative study on rice husk, as agricultural waste, in the production of silica nanoparticles *via* different methods," *Materials* 17(6), article 1271. https://doi.org/10.3390/ma17061271

Yusof, M. Y. M., and Abu Bakar, M. A. (2025). "Optimizing silica extraction form rice ash: A comparative study of alkaline and acid leaching," *Scientific Research Journal* 22(Special Issue), 91-105. https://doi.org/10.24191/srj.v22is.12353

Yuvakkumar, R., Elango, V., Rajendran, V., and Kannan, N. (2014). "High-purity nano silica powder from rice husk using a simple chemical method," *Journal of Experimental Nanoscience* 9(3), 272-281. https://doi.org/10.1080/17458080.2012.656709

Zainal, N. S., Mohamad, Z., Mustapa, M. S., Badarulzaman, N. A., Masirin, M. I., and Salim, Z. A. S. A. (2018). "Study of characteristics of rice husk and silica obtained from rice husk," *International Journal of Chemical Engineering and Applications* 9(5), 158-162. https://doi.org/10.18178/ijcea.2018.9.5.718

Zainal, N. S., Mohamad, Z., Mustapa, M. S., Badarulzaman, N. A., and Zulkifli, A. Z. (2019). "The ability of crystalline and amorphous silica from rice husk ash to perform quality hardness for ceramic water filtration membrane," *International Journal of Integrated Engineering* 11(5), 229-235. https://doi.org/10.30880/ijie.2019.11.05.029

Zarib, N. S. M., Abdullah, S. A., and Jamil, N. H. (2019). "Extraction of silica from rice husk *via* acid leaching treatment," in: *The European Proceedings of Social & Behavioural Sciences*, D. M. I. Qureshi, D. M. S. Malik, D. M. M. Khan, D. F. Jamil, and D. M. Yasir (eds.), Future Academy, Palo Alto, CA, USA, pp. 175-183. https://doi.org/10.15405/epsbs.2019.05.02.16

Zegzulka, J., Gelnar, D., Jezerska, L., Prokes, R., and Rozbroj, J. (2020). "Characterization and flowability methods for metal powders," *Scientific Reports* 10(1), article 21004. https://doi.org/10.1038/s41598-020-77974-3

Article submitted: January 5, 2026; Peer review completed: March 21, 2026; Revised version received: May 11, 2026; Accepted: June 5, 2026; Published: June 19, 2026.
DOI: 10.15376/biores.21.3.7192-7210